J. Coat. Technol. Res.
https://doi.org/10.1007/s11998-025-01231-3

# Water-based vs. organic solvent-based processing of NVP/C cathodes for sodium-ion batteries toward higher processing rates

**David Burger, Hanqing Sun, Xuebin Wu, Noah Keim, Marcus Müller, Werner Bauer, Helmut Ehrenberg, Philip Scharfer, Wilhelm Schabel**

Received: 28 March 2025 / Revised: 10 October 2025 / Accepted: 19 October 2025


**Abstract** Sodium-ion batteries are treated as a drop-in technology to complement lithium-ion batteries in applications such as entry-level cars and stationary storage. This study compares water-based processing of the sodium-ion battery active material sodium vanadium phosphate (NVP/C) with processing using slurries based on the organic solvent NMP. By utilizing CMC/SBR as a binder, the adhesion strength, flexibility, electrical resistance, and rate capability were improved. These superior properties could be maintained at increasing the drying rate by a factor of 8. However, electrodes processed with the water-based binder system also suffered from binder migration at higher drying rates. To enable high-throughput processing, a strategy involving simultaneous multilayer coating of a primer and electrode slurry was explored. This approach helped mitigate the negative effects of binder migration.

**Keywords** Sodium-ion batteries, Electrode processing, Microstructure optimization, Binder migration

This article is a contribution to the special issue on Li-ion battery electrode manufacturing.

D. Burger (✉), H. Sun, P. Scharfer, W. Schabel
Thin Film Technology (TFT), Karlsruhe Institute of Technology (KIT), Straße am Forum 7, D-76131 Karlsruhe, Germany
e-mail: david.burger@kit.edu

X. Wu, N. Keim, M. Müller, W. Bauer, H. Ehrenberg
Institute for Applied Materials (IAM), Karlsruhe Institute of Technology (KIT), Hermann-von-Helmholtz-Platz 1, D-76144 Eggenstein-Leopoldshafen, Germany

## Introduction

Sodium-ion batteries (SIBs) are becoming a pivotal energy storage solution to complement lithium-ion batteries (LIBs). SIBs can serve a growing demand for stationary electrochemical storage or mobility applications without high requirements on energy density. Through appropriate selection of active materials, they can achieve long cycle life and competitive charging performance.[1,2] Using the same process steps for electrode production as in LIBs, SIBs are handled mostly as a drop-in technology. However, to be competitive with lithium-ion batteries, it is necessary to keep the costs of the cells as low as possible. Besides raw material cost, prospective cost reductions for electrodes are possible by increasing the drying rate during electrode production and thus having a higher throughput or decreased investment and operating cost by shorter dryers.[3] However, already in LIB, elevated drying rates pose challenges to electrode adhesion, among issues with diminished C-rate capability due to binder migration during drying.[4,5]

Component migration during convective transport in the capillary system of a drying porous electrode is inevitable, especially if the binder is dissolved in the solvent, like polyvinylidene fluoride (PVDF) in N-methyl-2-pyrrolidone (NMP). The usage of PVDF is still widespread in the scientific community, as well as industrial cathode electrode production for lithium-ion batteries. In research, it is often the starting point to develop or benchmark slurry formulations, e.g., for sodium-ion batteries. However, benefits of SIBs regarding material abundancy and low-cost processing rely on the ability for water-based processing: Processing with NMP is a unnecessary cost driver for the drying process due to solvent recovery,[6,7] if water-based processing is a feasible alternative.

Regarding water-based processing, Klemens et al. showed the general challenges associated with large-

Published online: 20 March 2026

scale electrode processing for SIBs, particularly in terms of coating and drying, when compared to LFP and graphite.[3] Especially for most SIB cathode materials having a lower specific discharge capacity than LFP (< 165 mAh $g^{-1}$)[8], thicker layers and higher drying rates become necessary to keep production costs low. However, either increasing the thickness or faster drying can lead to more binder migration and limit the C-rate capability.[4,9,10] By using water-based binder systems of sodium carboxymethyl cellulose (CMC) and styrene–butadiene rubber (SBR) together with structural optimization on the active material or electrode level, the binder migration can be mitigated to a certain extent.[11,12] This has already been demonstrated for SIB anodes made of hard carbon[11] as well as examples from LIBs, through strategies like high-intensity mixing,[13] additive usage,[12] or structural optimization by simultaneous multilayer coating.[14] With these opportunities given, in this work, the direct transfer of a CMC/SBR binder system to a new material is explored in comparison to processing with PVDF.

### *Water-based processing of SIB CAM materials*

From an economical point of view, it is beneficial to process slurries with water rather than NMP, as solvent recovery from the exhaust dryer air is not obligatory and the requirements for explosive atmosphere protection of the drying equipment are less stringent.[6,7] However, water-based processing of cathode active material (CAM) in LIB and SIB technology is limited to active materials that are—or are made—chemically stable in water. Layered oxides used in both SIBs and LIBs require careful moisture management because they react with $H_2O$ and $CO_2$ in contact with humid air.[15] Direct contact with liquid water can also be problematic, causing ion leaching from the material, altering the slurry pH, and promoting corrosion of the aluminum substrate.[16] Treating the surface of CAM with protective coatings can reduce these issues.[17] However, additional effort must always be weighed against the superiority of these materials regarding the energy density of electrodes.

There are more stable active materials, like lithium iron phosphate (LFP) for LIBs,[18] that can be directly processed with water. Thus, it is the main competitor for SIBs in terms of production of low-cost cells for energy storage applications. A direct transfer to sodium-iron phosphate (NFP) may be possible. However, there are strong alterations of the known, flat voltage profile of LFP for using NFP.[19] Sodium vanadium phosphate $Na_3V_2(PO_4)_3$ is a promising polyanionic SIB cathode material that allows for a flat, comparable voltage profile at $\sim$ 3.4 V vs. Na+ /Na for NVP/C. This transferability leads to a high interest in the literature.[20–27] However, there is little information about processing the material with water-based slurries,[20,28] especially none for commercially available materials.

NVP, like LFP, has the disadvantage of low electronic conductivity. Therefore, it is usually used with a carbon matrix or coating (NVP/C).[20,22–27] Other than using small particles with surface coating, NVP can be processed into spherical secondary particles, filled with a carbon component to overcome the poor electrical conductivity of the material. Additionally, smaller primary particles and the open porous structure (44.9 % inside particle porosity) lead to short pathways for sodium diffusion inside the CAM and make it stable against material cracking during cycling.[5,22,23,29] For these structures, water-based processing with a mixture of CMC/SBR and polyacrylic acid (PAA) has been reported in literature.[20]

## Experimental

NVP electrodes were prepared either by water-based processing with CMC/SBR or by organic solvent-based processing with PVDF in NMP. Their suitability for high-throughput electrode fabrication was evaluated by systematically increasing the drying rate and comparing their mechanical and electrochemical properties.

### *Materials and mixing*

Cathode active material NVP/C (TOB-NVP/C, Xiamen TOB New Energy Technology Co. Ltd., China) with a shard-like particle morphology was used, as shown in Fig. 1. The material was sieved with a 50 µm sieve resulting in a monomodal particle size distribution with $x_{50}$ of 7.5 µm (LA-950, Horiba, Japan). A field emission scanning electron microscope (Zeiss Supra 55, Carl Zeiss AG, Germany) was used to obtain the SEM micrograph (SE2, 2 kV).

A significant amount of carbon black is incorporated as a partial surface coating. Inductively coupled plasma–optical emission spectroscopy (ICP–OES, iCAP 7600 Duo, Thermo Fisher Scientific) determined a carbon content of 3.22 wt-%. For sample preparation, the material was dissolved with acid in a graphite furnace and the resulting solution was filtered and subsequently acidified.

Using NVP/C as the active material, slurries were prepared in a dissolver (Dispermat SN-10, VMA Getzmann GmbH Verfahrenstechnik, Germany) with cooled container. For water-based slurry preparation, carbon black (Super C65, Imerys Graphite & Carbon Ltd., Switzerland) and an additional conductive additive (KS6L, Imerys Graphite & Carbon Ltd., Switzerland) were dispersed in a 2 wt-% CMC solution (Sunrose MAC500LC, Nippon Paper Industries, Japan) at 1500 rpm for 30 min. The active material particles were added afterward as well as further water

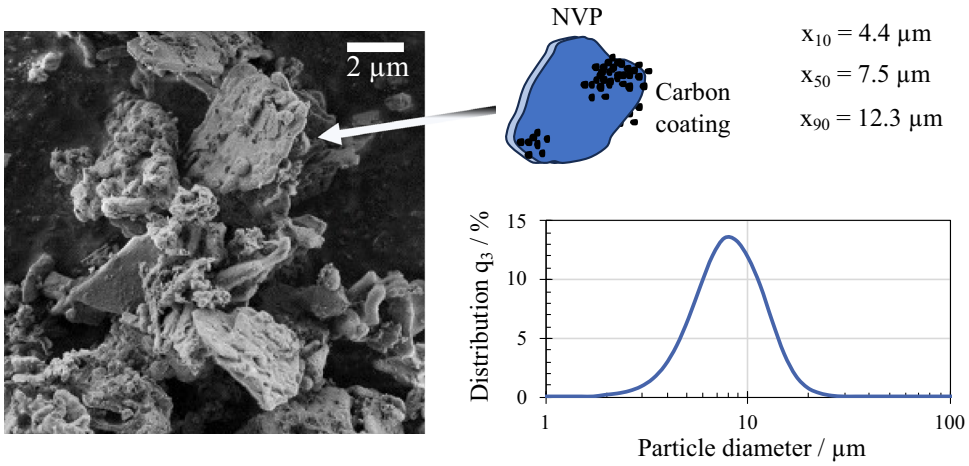


**Fig. 1: SEM micrograph of the active material. Shard-like particles of NVP are agglomerated by carbon black (NVP/C) to structures of ~ 4–12 µm ($x_{10}$–$x_{90}$)**

**Table 1: Composition of electrode slurry with 43 wt% solid content**

| | C65 / wt-% | KS6L / wt-% | CMC / wt-% | SBR / wt-% | PVDF / wt-% | NVP/C / wt-% |
|---|---|---|---|---|---|---|
| Water-based slurry "CMC/SBR" | 3 | 2 | 2 | 2.5 | – | 90.5 |
| NMP slurry "PVDF" | 3 | 2 | – | – | 4.5 | 90.5 |

for the final solid content. The slurries were then homogenized for further 30 min at 1500 rpm. In the final step, SBR (Zeon Europe GmbH, Japan) was added as aqueous dispersion and the slurry was mixed for 10 min at 500 rpm and degassed. For NMP-based slurry preparation PVDF (Solef 5130, Solvay S.A., Belgium) was used as binder and NMP (>99.8 %, Carl Roth, Germany) as solvent. The mixing protocol included the same two-step dispersion procedure starting from a 7.5 wt-% PVDF solution.

Table 1 provides an overview of the coating slurries formulations made with either water or NMP as solvent. The total mass fraction of binder, solvent and conductive additives remains constant when switching from NMP-based to water-based processing. In the case of water-based processing, the 4.5 wt-% of PVDF used in NMP-based processing are replaced by 2 wt-% CMC, serving as a dispersing and thickening agent, and 2.5 wt-% SBR, which reduces electrode stiffness and improves adhesion.

After slurry preparation, the viscosity was measured by a rotational viscometer (Physica MCR 101, Anton Paar, Germany) with a plate–plate geometry (25 mm diameter) from 0.01 − 1.000 $s^{-1}$ at 25 °C. Additionally to the slurries, comparison mixtures of only solvent and binder ($H_2O$+CMC/SBR and NMP+PVDF) as well as of solvent, binder, and conductive additives ($H_2O$+CMC/SBR+C65+KS6L and NMP+PVDF+C65+KS6L) were prepared and their flow curve measured. The concentrations in the comparison mixtures were calculated by the following equation:

$$x_{\mathrm{i,comparisonmixture}} = x_{\mathrm{i,slurry}} \frac{x_{\mathrm{solidcontent}}}{1 - x_{\mathrm{solidcontent}}}$$

### *Electrode coating and drying*

Coating and drying of the NVP/C electrodes were carried out in a discontinuous process as described by Baunach et al.[30] using a 16-µm-thick aluminum current collector (Xiamen TOB New Energy Technology Co. Ltd., China). While coating and drying the substrate was attached to a temperature-controlled plate via vacuum. The slurries were applied with a doctor blade ZUA 2000.60 (Zehntner GmbH, Switzerland), and subsequently, the electrode was coated under the drying nozzles of an impingement dryer. For homogeneous drying, the plate was periodically moved under the dryer until the slurry was dry. The drying temperature and heat transfer coefficient were set independently to separate their respective effects. For all experiments, the drying rate was set by adjusting the temperature of the heated plate and the drying air considering its dew point. Table 2 shows the drying rates with the corresponding sets of heat transfer coefficient and drying temperature.

**Table 2: Overview of the drying rates and the drying temperatures with a constant heat transfer coefficient of 35 W $m^{-2}$ $K^{-1}$ for water and 83 W $m^{-2}K^{-1}$ for NMP. The dew point during the experiments ranged from −1 to 14 °C. In case of water as a solvent, the drying temperature was set according to the dew point on the experiments´ day. For each solvent, a lower drying rate (LDR) and a higher drying rate (HDR) are compared**

| | Drying rate / g $m^{-2}$ $s^{-1}$ | Heat transfer coefficient / W $m^{-2}$ $K^{-1}$ | Film temperature (range) / °C |
|---|---|---|---|
| LDR water | 0.75 | 35 | 27.6 - 31.7 |
| HDR water | 6 | 35 | 62.7 - 63.4 |
| LDR NMP | 0.75 | 83 | 61 |
| HDR NMP | 3.5 | 83 | 89 |

As the vapor pressure of NMP and water and their temperature dependency vary, for the drying investigation the same lower drying rate (LDR) was used as a starting point for comparison of the two slurry systems. A higher drying rate (HDR) was achieved by increasing the drying temperature by 30 °C, respectively. With this, the drying rate increases from 0.75 g $m^{-2}$ $s^{-1}$ to 3.5 g $m^{-2}$ $s^{-1}$ in case of NMP and to even 6 g $m^{-2}$ $s^{-1}$ in case of water. The shift from LDR to HDR is intended to characterize the ability of the material system to withstand binder migration and being processed at high throughput.

### *Electrode characterization*

To mechanically characterize the electrodes, the adhesion strength between the current collector and the dried electrodes was determined in a 90° peel test by a universal testing machine (AMETEK LS1, Lloyd Instruments Ltd., UK) equipped with a 10 N load cell. As samples, the dried cathodes were cut out with a width of 30 mm and attached with the coated side to an adhesive strip. The sample was pressed on by rolling once with a cylindrical weight of 10 kg to ensure uniform contact between the coating and the adhesive strip. The current collector was then peeled off the coating by the testing machine at a constant speed of 600 mm $min^{-1}$ under a 90° angle. The pull-off force was measured and divided by the sample width to obtain a line force.

For all further characterization, already calendered samples were used (min to max // 47–50 % porosity). A mandrel bending test was conducted by bending electrode samples by hand around cylindrical mandrels (30 mm stripes, mandrel diameter 15 mm, 7 mm, and 3 mm). The sample was observed afterward for defects (no defect attributed by ''3'') like visible cracks (attributed by ''2'') or delamination of the electrode from the substrate (attributed by ''1''). For characterizing the electrical resistance of the electrodes, an electrode resistance measurement system (RM2610, HIOKI, Japan) was used.

**Table 3: Cycling protocol for full cell coin cell tests. C-rate capability (1–50) with afterward symmetrical long-term cycling at 1C (51–100)**

| Cycle | C-rate charge | C-rate discharge |
|---|---|---|
| 1–2 | 0.05 | 0.05 |
| 3–7 | 0.5 | 0.5 |
| 8–27 | 1 | 1, 2, 3, 4, 5 (5 cycles) |
| 27–48 | 1 | 1 |
| 49–50 | 0.05 | 0.05 |
| 51–100 | 1 | 1 |

### *C-rate capability tests*

The calendered cathodes (16 mm diameter) were electrochemically examined in coin full cells (CR 2032, Hohsen, Japan) against a hard carbon (HC) counter electrode (KURANODE Type II 9 μm, Kuraray Co., Ltd., Japan) with N/P-ratio of 1.2 (assuming HC specific capacity of 335 mAh $g^{-1}$). Foregoing the assembly of the cells, the electrodes were post-dried in a vacuum oven (130 °C, 16 h) to evaporate residual moisture. The electrolyte used was 1 M $NaPF_6$ in a mixture of ethylene carbonate and propylene carbonate (EC/PC 1/1 w/w).[23] As separator, a glass microfiber fleece (Whatman GF/C, cytiva, US) was used. The cells were assembled in an argon-filled glovebox and sealed using a MSK-11 press (MTI Corporation, US). Cycling was carried out in constant current mode (CC) within a voltage range of 2.3–3.9 V. The cycling protocol is given in Table 3.

## Results and discussion

In this work, water-based slurry processing is compared to NMP-based processing. By a characterization of electrodes, which are dried with increasing drying rate it is investigated which binder system, CMC/SBR (water-based slurry) or PVDF (NMP-based slurry), is more applicable for fast processing of NVP/C electrodes. For the water-based processing, a microstruc-

ture optimization by simultaneous primer coating is discussed further.

### *Slurry comparison*

Prior to characterizing electrodes, differences in slurry processing for the different solvents, water or NMP, must be evaluated, because slurry properties impact processing during coating and drying. Figure 2 shows the viscosity of the slurries obtained by shear rheometry after the slurry production.

It becomes apparent that the viscosity of the NMP-based slurry ''PVDF'' is orders of magnitude higher compared to the water-based slurry ''CMC/SBR.'' The high viscosity originates mostly from particle–particle interaction with an increasing viscosity and shear-thinning behavior adding conductive additives (NMP+PVDF+C65+KS6L) and NVP/C to the slurry, respectively. For comparison, NMP with only the binder PVDF (NMP+PVDF) shows almost no shear-thinning behavior. In contrast to that, the water-based slurry without particles ($H_2O$+CMC/SBR) already shows a viscosity over one order of magnitude higher in the lower shear rate range as well as a more pronounced shear-thinning behavior due to the thickening function of CMC. Adding the conductive additives ($H_2O$+CMC/SBR+C65+KS6L), the viscosity is comparable to the NMP slurry without NVP/C (NMP+PVDF+C65+KS6L). However, after adding the NVP/C particles the viscosity of the water-based slurry drops. For the water-based slurry, the viscosity is reaching a viscosity as little as 0.2 Pa s in the higher shear rate rage between 100 and 1000 $s^{-1}$ and its shear-thinning behavior in this range is almost lost. This suggests that a strong interaction between the thickener CMC and the particle surface exists in the water-based slurry, leading to less free polymer in the solvent and hence less thickening. Corresponding with the low viscosity, issues with sedimentation of the slurry were avoided by coating in a time window of few hours after production. However, for further formulation development, the use of more CMC[31] than in this work as well as the use of alternative binder or a co-thickener by a combination of CMC/SBR and PAA[20] might be considered.

Other than the viscosity of the slurry, the pH value and stability of NVP/C in demineralized water are to be evaluated for the water-based processing. A water suspension with a small amount of NVP/C (9 $g_{Water}$ / $g_{NVP/C}$) was made with demineralized water. The pH of the suspension was measured over time. Figure 3 shows the pH value vs. the immersion time as well as the pH values during the slurry preparation.

Directly after preparation of the suspension, the sample has a pH of 6.1. The pH decreases with time to a boundary value of 5.8 measured after 48 h. Most of the shift happens in the first hour of the experiment. The presence of a blue–green tint of the water after some time indicates the presence of $V^{3+}$.[32] There is only a slight decrease in pH with immersion time, which could also be a result of absorption of $CO_2$ from the surrounding air in the demineralized water. In case of the slurry, the pH level drops from 7.5 for the CMC solution to 6.5 for the final slurry. This pH level during electrode processing is beneficial, because corrosion of the aluminum current collector is suppressed in the pH range from 4.5 to 8.5,[33] while it can be problematic for, water-based processing of LIBs which happens at elevated pH (e.g., pH > 10 for NCM111 in water).[34]

### *Drying study*

Competitiveness of NVP/C to other cathode materials relies among the ability for being processed in water-based slurries also on the processing speed during coating and drying. The adhesion strength is a first indicator to determine whether the electrode quality is compromised by migration of binder due to an

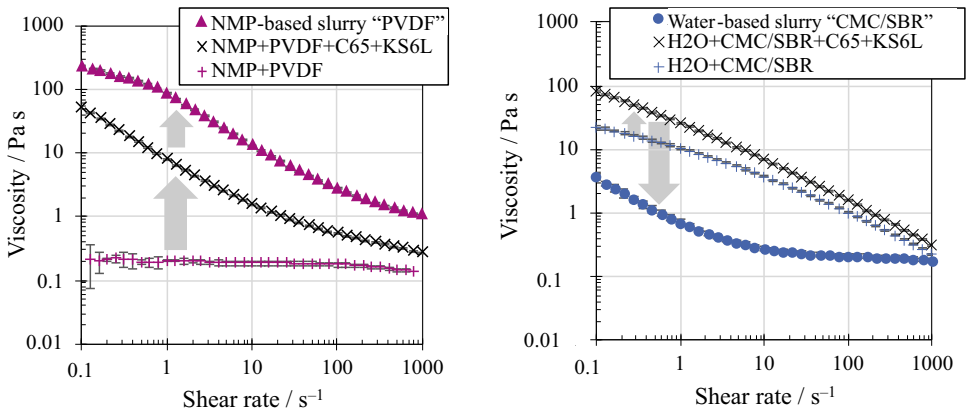


**Fig. 2: Flow curve as viscosity vs. shear rate for the NMP-based slurry ''PVDF'' (left) as well as the water-based slurry ''CMC/SBR'' (right). To show the influence of conductive additives as well as active material particles on the slurry viscosity, the flow curves of the same mixtures are shown without adding NVP/C (solvent, binder, conductive additives) and those without adding particles at all (solvent, binder) are shown**

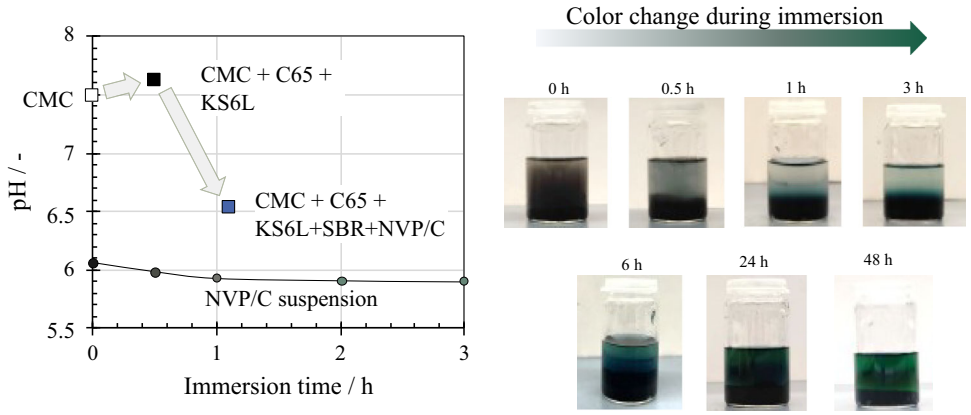


**Fig. 3: pH of NVP/C suspension in demineralized water in the processing time window (3 h) and longer-term period (6–48 h, just images) as well as color change visible in the suspension**

increased drying rate. In Fig. 4 (left), the adhesion strength (90°-peel test) is shown vs. the drying rate of the sample for NVP/C electrodes with an areal capacity of 0.89–1.02 mAh $cm^{-2}$ (min to max) made with the NMP-based slurry "PVDF" as well as with the water-based slurry "CMC/SBR." For determining whether winding is a limitation for the formulations, Fig. 4 (right) complements the adhesion strength with a characterization by a cylindrical mandrel bending test with roll diameters from 3–15 mm.

Both systems indicate an impact of fast processing on the electrode microstructure by the drop in adhesion strength by increasing the drying rate which falls in line with the literature on the influence of drying temperature on both water-based as well as NMP-based battery electrodes.[9,35] Besides that, the electrodes with the water-based binder system CMC/SBR (containing the same wt-% of binder and thickener in total) show a generally higher adhesion strength. Even twice the increase in the drying rate by increasing the drying temperature by 30 °C still leads to a higher adhesion strength compared to PVDF. The superior performance of water-based binder systems compared to equivalent amounts of PVDF aligns with the literature on LIB processing.[36] Further, the mandrel bending test shows that both binder systems generally show processability in a roll-to-roll process. However, at small mandrel diameters cracks start to show for the PVDF HDR electrodes already at 7 mm, whereas for the CMC/SBR HDR electrodes cracks show due to mandrel bending at 3 mm.

Characterizing the contact between electrode and current collector with another measurement technique, the electrical interface resistance (in Ohm $cm^2$) is shown over the drying rate in Fig. 5.

For both binder systems, there is a clear trend of increasing interface resistance with increasing the drying rate, which is in accordance with literature.[37,38] The trend falls in line with the decreasing adhesion strength at higher drying rates. In both cases, this can be explained by capillary transport of solvent during pore emptying reducing not only the amount of binder

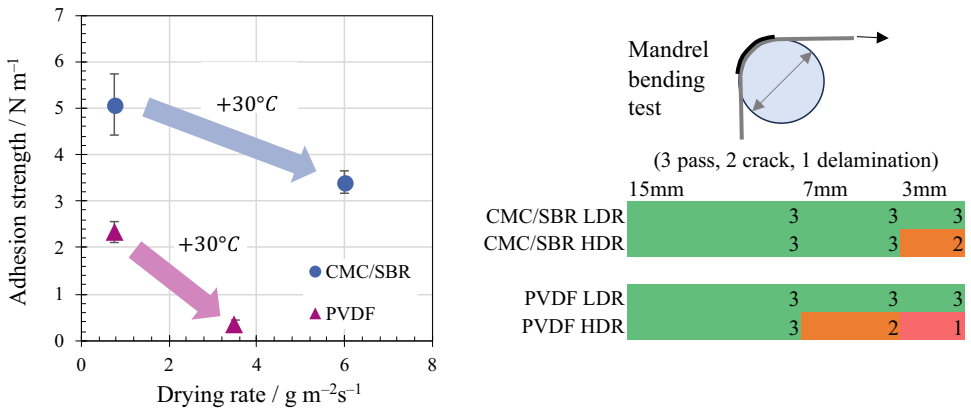


**Fig. 4: Adhesion strength quantitatively (left) and mandrel bending test (right) vs. the drying rate of electrodes made with water-based processing binder system CMC/SBR and NMP-based processing binder PVDF at same total binder concentration. For the electrodes made with PVDF, visible crack formation (attributed with "2") and delamination (attributed with "1") occur at higher mandrel diameter. For CMC/SBR, most samples pass the bending test without cracking (attributed with "3")**

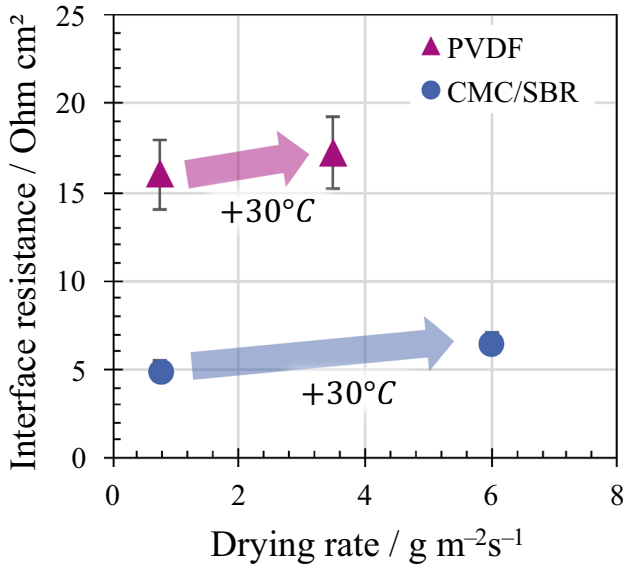


**Fig. 5: Interface resistances vs. the drying rate of calendered samples of the NVP/C electrodes made with PVDF or CMC/SBR. Inversely to the adhesion strength, the interface resistance increases with increasing drying rate**

but also of carbon black at the interface with the current collector.

To compare the quality of the electrodes made with the two processing variants regarding their performance, C-rate capability tests were conducted in coin cells that were built as full cells against hard carbon (HC) anodes. In Fig. 6 the specific discharge capacity for increasing C-rate is compared between electrodes made with the slurries "PVDF" or "CMC/SBR" and drying them at a lower drying rate (LDR) or higher drying rate (HDR).

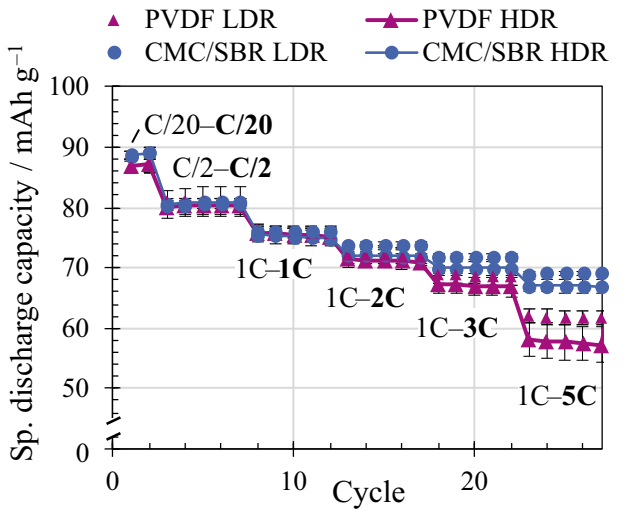


**Fig. 6: C-rate capability test for water-based "CMC/SBR" and NMP-based "PVDF" slurries. A lower drying rate (LDR) is compared to a higher drying rate (HDR), respectively**

The initial specific discharge capacity is in the range of 85.7–89.4 mAh $cm^{-2}$ (min to max) for both binder systems with overlapping error bars (deviation of three cells, respectively). No drop in specific capacity due to the water-based processing could be shown. Difference to the specific discharge capacity of NVP/C (110 mAh $g^{-1}$ vs. Na metal) is due to irreversible sodium losses to hard carbon during cell formation.[23] After formation, the capacity of all samples drops according to the overpotential assigned by the ionic and electric resistances of the respective electrode's microstructures. Both systems show the binder migration typical drop in specific capacity comparing LDR and HDR samples at increasing C-rate. Especially at 5C, a similar trend from adhesion strength measurements becomes visible in the cell. The LDR samples are outperforming the HDR samples that are impaired by binder migration. In the C-rate range from 2–5C, the samples made with CMC/SBR can offer benefits compared to PVDF. For the C-rates 2–5C, the sample HDR for CMC/SBR outperforms the PVDF sample LDR even though it was dried 8 times faster.

In Fig. 7, additional longer-term cycles with symmetric charge and discharge C-rate are shown for the electrodes processed with PVDF or CMC/SBR for a lower drying rate (left) or higher drying rate (right). The tests are subsequently to the cell tests shown in Fig. 6 using the same cells.

From the measurements, it can be concluded that the ionic transport resistances due to binder migration become apparent also under longer-term cycle stress and that they are less in the CMC/SBR electrodes. The CMC/SBR electrodes are as well able to regain more of the specific capacity in the C/20–C/20 check-up cycles 49 and 50. As the binder content is shared between a polymer matrix (CMC) and point contacting SBR,[39] the effective tortuosity is supposedly smaller for the water-based processing. However, by binder migration at increased drying rate the cell performance deteriorates too. For the NMP-based processing, the results of a stronger migration behavior for adhesion strength, conductivity, and handling experience are met by the electrochemical characteristics. Hence, to achieve higher drying rates, water-based binder systems offer a wider range of opportunities for optimization than PVDF and further research should focus on water-based binder systems not only from an ecological but also economical and quality-related point of view.

### *Microstructure optimization*

Having shown that water-based processing is possible but still dealing with binder migration at increased drying rates, the processing of NVP/C with the binder system CMC/SBR offers the opportunity for microstructure optimization by simultaneous primer coating. The approach was previously presented by the authors for faster drying of graphite anodes.[37] By

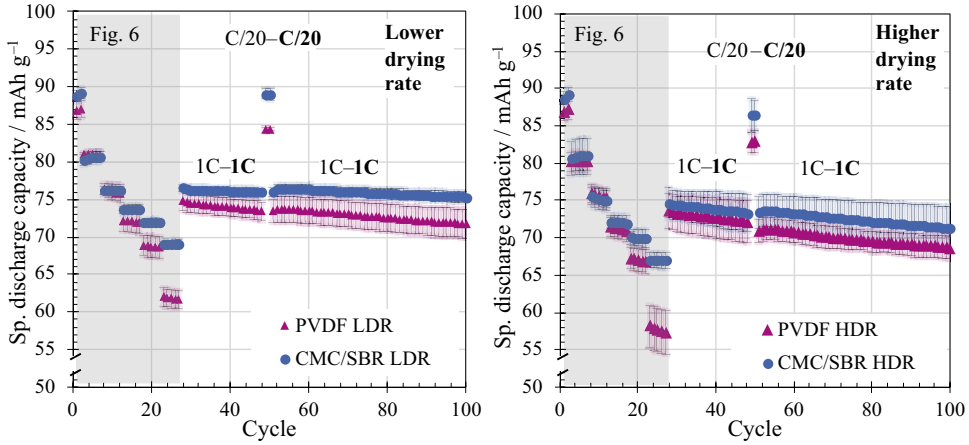


**Fig. 7: Symmetric longer-term cycle tests for electrodes made with the water-based "CMC/SBR" and NMP-based "PVDF" slurry. Electrodes dried at a lower drying rate (LDR, left) are compared to electrodes dried at a higher drying rate (HDR, right), respectively**

concentration of the SBR in a thin primer layer that is applied simultaneously to the electrode slurry, binder migration can be buffered and benefits for C-rate capability can be gained. Even electrodes with just CMC as binder (no SBR in electrode slurry) are achievable. Transferring the approach to other active materials, in case of NVP/C, especially the high interface resistance compared to graphite anodes is of interest. For the simultaneous multilayer coating, two doctor blades were joined. The primer slurry "Primer" was prepared according the water-based slurry with a solid content of 5.4 wt-% composed of 18.75 wt-% C65, 25 wt-% CMC, 50 wt-% SBR and 6.25 wt-% of the additive Laponite® RD. Additionally, an SBR-free slurry "CMC" (93 wt% NVP/C, 3 wt-% C65, 2 wt-% KS6L, 2 wt-% CMC) was made aiming for a higher active material share and lower ionic resistance. With a thickness of $\sim 2$ µm and coating weight of $\sim 2$ g m$^{-2}$, the primer has a share of $\sim 2$ wt-% of the areal mass loading leading to an estimated reduction of SBR content by at least 50% compared to the formulation "CMC/SBR" without primer. In Fig. 8, the characterization of electrodes made with the slurry "CMC/SBR," the slurry "CMC" as well as a multilayer composed of the slurry "CMC" simultaneously coated onto the slurry "Primer" is shown. The samples were dried with the higher drying rate (HDR). The characterization includes (A) adhesion strength, (B) interface resistance, and (C) C-rate capability (full cells in coin cell format according to Fig. 6).

The adhesion strength measurement shows a drop in adhesion strength if SBR is removed from the formulation. The use of the primer increases the peel strength. However, a delamination between the primer and the electrode coating is limiting. Such an interlayer delamination has already been shown for simultaneous primer coatings for graphite anodes for LIB.[37] Only the electrodes made with CMC/SBR and a combination of the CMC slurry with the primer could be cut for their testing in coin cells after calendering. The electrodes with just CMC showed delamination during the electrode cutting. The issue that electrode stiffness can become a problem with reduction of the SBR content[40] could be validated.

For the electric conductivity, an inverse effect was observed. Compared to the better adhering electrodes made with "CMC/SBR," the electrodes made with "CMC" showed a lower interface resistance. It can be argued that better mechanical contact by using SBR does not ensure electrical contact, as it still is isolating material. Using the primer that contains besides binder as well a high proportion of C65, the interface resistance can be reduced significantly. The amount of C65, with the same mass ratio between SBR and C65 as in the electrode formulation, is sufficient to provide a highly conducting network throughout the primer as well as electrical connection to the active material coated on top of it. This effect has been shown before in graphite anodes using binder system CMC/SBR as well as just CMC in combination with the same primer. However, it was much less pronounced as the electrical resistances of graphite anodes are generally lower by orders of magnitude.[37]

For the cell tests, the use of less SBR binder is expected to increase the C-rate capability.[40] Using SBR binder just in the primer layer, the C-rate capability of the NVP/C electrodes made with the slurry "CMC" could be improved. Both less binder in the system and the reduced electrical interface resistance benefit the C-rate capability.

By the three complementary characterization methods, the structure optimization by the simultaneous primer coating is shown for another use case than for graphite anodes. Besides facilitating higher drying rates by introducing SBR binder just in the bottom layer of simultaneously coated primer and electrode, the approach makes processing of formulations feasible that would not be processable in a single-layer

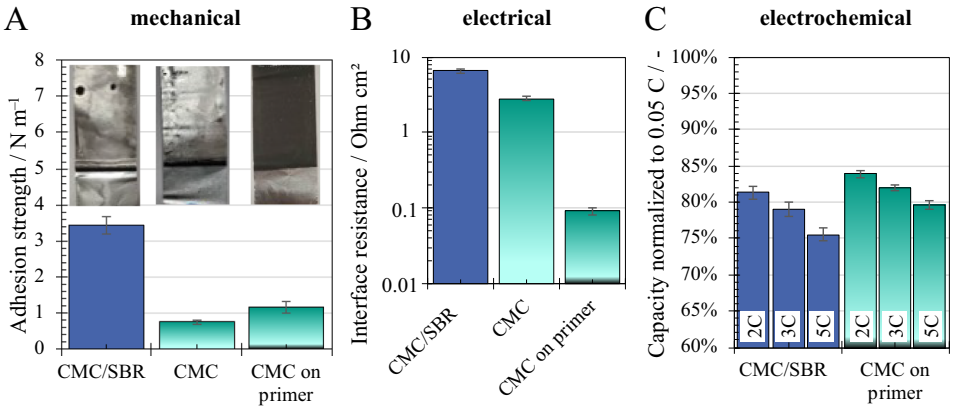


**Fig. 8: (A) Adhesion strength with photo of the residue on current collector after peel test and (B) interface resistance of NVP/C electrodes prepared with slurries "CMC/SBR," "CMC," and a multilayer of "Primer"+"CMC" under fast drying (HDR) conditions. (C) Capacity retention (average over 5 cycles, normalized to the second cycle discharge) at different C-rates is shown for the single-layer "CMC/SBR" electrode and "CMC" electrode simultaneously coated on the primer**

coating. For demanding materials, this offers another degree of freedom in microstructure optimization.

## Conclusions

In this work, processing of NVP/C with NMP/PVDF and water-based processing with CMC/SBR were compared according to the development of their mechanical properties (adhesion strength), electrical conductivity (interface resistance), and electrochemical performance (C-rate test with subsequent symmetric longer-term 1C cycles) with increasing drying rate. The water-based binder system offers a higher adhesion strength, lower resistance as well as superior C-rate capability. Even dried at a higher drying rate HDR (8x faster drying), where migration of binder impairs the C-rate capability of the electrodes, they were still superior to electrodes processed with PVDF binder. However, the electrodes made with CMC/SBR are affected by binder migration as well. By using the water-based processing in combination with a simultaneously coated primer layer, it was possible to further improve the electrodes and reduce the amount of SBR in the electrode by approximately 50%. With the simultaneous primer, processing of a slurry without SBR in the electrode slurry was feasible.

However, one disadvantage of the water-based processing was relatively low viscosity, complicating slurry handling due to the possibility of sedimentation. Given these results, further optimization of NVP/C electrodes for sodium-ion batteries should focus on water-based processing but must consider some boundaries:

- **Provision of adhesion, cohesion/elasticity:** Either by sufficiently high SBR binder content (on cost of C-rate capability) or by microstructure optimization by multilayer approaches. The results suggest that SBR should be present at least in the bottom layer of the electrode.
- **Processability:** A co-thickener might be necessary for water-based processing if the interaction of particles with CMC is reducing the viscosity to an undesirable value in terms of stability against sedimentation or for coating. It must be noted that other NVP/C with porous morphologies show a higher specific surface area.[23] The interaction of polymer with the particle surface and thus reduction of viscosity might scale with the surface area of the particles making further development of water-based formulations necessary.

**Acknowledgments** During the drafting of this article, large language models were used. While the model was used to aid in ensuring readability, all data analysis, interpretations, conclusions, and final edits were made by the authors. The authors take full responsibility for the accuracy, validity, and originality of the content presented. This work contributes to the research performed at CELEST (Center for Electrochemical Energy Storage Ulm Karlsruhe) and Material Research Center for Energy Systems (MZE). It was funded by the Deutsche Forschungsgemeinschaft (DFG, German Research Foundation) under Germany's Excellence Strategy—EXC 2154—Project number 390874152 (POLiS Cluster of Excellence). The authors would like to thank M. Raab (IAM) for particle size analysis, Th. Bergfeldt (IAM) for performing the ICP–OES as well as A. Hofmann (IAM) for electrolyte preparation.

**Funding** Open Access funding enabled and organized by Projekt DEAL. Deutsche Forschungsgemeinschaft, EXC 2154 – Project number 390874152

**Data availability** The authors declare that the data supporting the findings of this study are available within the paper. Additional data and metadata are available in the Zenodo repository with the https://doi.org/10.5281/zenodo.15082934

## References

1. Titirici, M, Adelhelm, P, Hu, Y-S (eds.) *Sodium-Ion Batteries*. Volume 1. Wiley-VCH, Weinheim (2023)
2. Fraunhofer-Institut für Solare Energiesysteme ISE. ResHy – Ressourcenschonende Hybridbatterie. *Fraunhofer-Institut für Solare Energiesysteme ISE* https://www.ise.fraunhofer.de/de/forschungsprojekte/reshy-ressourcenschonende-hybridbatterie.html (2022, access 30.09.2024).
3. Klemens, J, et al. ''Challenges and Opportunities for Large-Scale Electrode Processing for Sodium-Ion and Lithium-Ion Battery.'' *Batter. Supercaps*, **6** (2023)
4. Müller, M, et al. ''Investigation of Binder Distribution in Graphite Anodes for Lithium-Ion Batteries.'' *J. Power Sources*, **340** 1–5 (2017)
5. Klemens, J, et al. ''Drying of NCM Cathode Electrodes with Porous, Nanostructured Particles Versus Compact Solid Particles: Comparative Study of Binder Migration as a Function of Drying Conditions.'' *Energy Technol.*, **10** 2100985 (2022)
6. Wood, DL, et al. ''Technical and Economic Analysis of Solvent-Based Lithium-Ion Electrode Drying with Water and NMP.'' *Dry. Technol.*, **36** 234–244 (2018)
7. Ahmed, S, Nelson, PA, Gallagher, KG, Dees, DW, ''Energy Impact of Cathode Drying and Solvent Recovery During Lithium-Ion Battery Manufacturing.'' *J. Power Sources*, **322** 169–178 (2016)
8. Baumann, M, et al. ''Prospective Sustainability Screening of Sodium-Ion Battery Cathode Materials.'' *Adv. Energy Mater.*, **12** 2202636 (2022)
9. Kumberg, J, et al. ''Drying of Lithium-Ion Battery Anodes for Use in High-Energy Cells: Influence of Electrode Thickness on Drying Time, Adhesion, and Crack Formation.'' *Energy Technol.*, **7** 1900722 (2019)
10. Jaiser, S, et al. ''Investigation of Film Solidification and Binder Migration During Drying of Li-Ion Battery Anodes.'' *J. Power Sources*, **318** 210–219 (2016)
11. Klemens, J, et al. ''Process and Drying Behavior Toward Higher Drying Rates of Hard Carbon Anodes for Sodium-Ion Batteries with Different Particle Sizes: An Experimental Study in Comparison to Graphite for Lithium-Ion-Batteries.'' *Energy Technol.*, **11** 2300338 (2023)
12. Burger, D. et al. ''Additive Influence on Binder Migration in Electrode Drying.'' *Energy Technol.,* **12** 2400057 (2024)
13. Kumberg, J, et al. ''Reduced Drying Time of Anodes for Lithium-Ion Batteries through Simultaneous Multilayer Coating.'' *Energy Technol.*, **9** 2100367 (2021)
14. Diehm, R, et al. ''In Situ Investigations of Simultaneous Two-Layer Slot Die Coating of Component-Graded Anodes for Improved High-Energy Li-Ion Batteries.'' *Energy Technol.*, **8** 1901251 (2020)
15. Zuo, W, et al. ''Layered Oxide Cathodes for Sodium-Ion Batteries: Storage Mechanism, Electrochemistry, and Techno-economics.'' *Acc. Chem. Res.*, **56** 284–296 (2023)
16. Çetinel, FA, Bauer, W, ''Processing of Water-Based $LiNi_{1/3}Mn_{1/3}Co_{1/3}O_2$ Pastes for Manufacturing Lithium Ion Battery Cathodes.'' *Bull. Mater. Sci.*, **37** 1685–1690 (2014)
17. Hofmann, M, Nagler, F, Kapuschinski, M, Guntow, U, Giffin, GA, ''Surface Modification of $LiNi_{0.8}Co_{0.15}Al_{0.05}O_2$ Particles via $Li_3P_O4$ Coating to Enable Aqueous Electrode Processing.'' *ChemSusChem*, **13** 5962–5971 (2020)
18. Li, J, Armstrong, BL, Daniel, C, Wood, DL III, ''Aqueous Processing of Composite Lithium Ion Electrode Material.'' US Patent US8956688B2 (2015)
19. Zhu, X, et al. ''A New Sodium Iron Phosphate as a Stable High-Rate Cathode Material for Sodium Ion Batteries.'' *Nano Res.*, **11** 6197–6205 (2018)
20. Mohsin, IU, Hofmann, A, Ziebert, C, ''Exploring the Rreactivity of $Na_3V_2(PO_4)_3$/C and Hard Carbon Electrodes in Sodium-Ion Batteries at Various Charge States.'' *Electrochim. Acta*, **487** 144197 (2024)
21. Jian, Z, et al. ''Carbon Coated $Na_3V_2(PO_4)_3$ as Novel Electrode Material for Sodium Ion Batteries.'' *Electrochem. Commun.*, **14** 86–89 (2012)
22. Stüble, P, et al. ''Enabling Long-term Cycling Stability of $Na_3V_2(PO_4)_3$/C *vs.* Hard Carbon Full-cells.'' *Batter. Supercaps*, **7** e202300375 (2024)
23. Stüble, P, et al. ''From Powder to Pouch Cell: Setting up a Sodium-Ion Battery Reference System Based on $Na_3V_2(PO_4)_3$/C and Hard Carbon.'' *Batter. Supercaps,* **7** e202300375 (2024)
24. Si, L, Yuan, Z, Hu, L, Zhu, Y, Qian, Y, ''Uniform and Continuous Carbon Coated Sodium Vanadium Phosphate Cathode Materials for Sodium-Ion Battery.'' *J. Power Sources*, **272** 880–885 (2014)
25. Shen, W, Wang, C, Liu, H, Yang, W, ''Towards Highly Stable Storage of Sodium Ions: A Porous $Na_3V_2(PO_4)_3$/C Cathode Material for Sodium-Ion Batteries.'' *Chem. Eur. J.*, **19** 14712–14718 (2013)
26. Huang, R, et al. ''Unlocking Charge Transfer Limitation in NASICON Structured $Na_3V_2(PO_4)_3$ Cathode via Trace Carbon Incorporation.'' *Adv. Energy Mater.*, **14** 2400595 (2024)
27. Akçay, T, et al. ''$Na_3V_2(PO_4)_3$—A Highly Promising Anode and Cathode Material for Sodium-Ion Batteries.'' *ACS Appl. Energy Mater.*, **4** 12688–12695 (2021)
28. Gu, Z-Y, et al. ''High-Rate and Long-Cycle Cathode for Sodium-Ion Batteries: Enhanced Electrode Stability and Kinetics via Binder Adjustment.'' *ACS Appl. Mater. Interfaces*, **12** 47580–47589 (2020)

29. Bauer, W, et al. ''Using Hierarchically Structured, Nanoporous Particles as Building Blocks for NCM111 Cathodes.'' *Nanomaterials*, **14** 134 (2024)
30. Baunach, M, Jaiser, S, Cavadini, P, Scharfer, P, Schabel, W, ''Local Heat Transfer Characteristics of a Slot Nozzle Array for Batch Drying of Thin Films Under Industrial Process Conditions.'' *J. Coat. Technol. Res.*, **12** 915–920 (2015)
31. Gordon, R, Orias, R, Willenbacher, N, ''Effect of Carboxymethyl Cellulose on the Flow Behavior of Lithium-Ion Battery Anode Slurries and the Electrical as Well as Mechanical Properties of Corresponding Dry Layers.'' *J. Mater. Sci.*, **55** 15867–15881 (2020)
32. Yue, J, et al. ''Interface Concentrated-Confinement Suppressing Cathode Dissolution in Water-in-Salt Electrolyte.'' *Adv. Energy Mater.*, **10** 2000665 (2020)
33. Bauer, W, Çetinel, FA, Müller, M, Kaufmann, U, ''Effects of pH Control by Acid Addition at the Aqueous Processing of Cathodes for Lithium Ion Batteries.'' *Electrochim. Acta*, **317** 112–119 (2019)
34. Hofmann, M, Kapuschinski, M, Guntow, U, Giffin, GA, ''Implications of Aqueous Processing for High Energy Density Cathode Materials: Part I. Ni-Rich Layered Oxides.'' *J. Electrochem. Soc.*, **167** 140512 (2020)
35. Westphal, BG, Bockholt, H, Gunther, T, Haselrieder, W, Kwade, A, ''Influence of Convective Drying Parameters on Electrode Performance and Physical Electrode Properties.'' *ECS Trans.*, **64** 57–68 (2015)
36. Binder, M, Keller, E, Bresser, D, ''Realization of High Mass Loading $LiNi_{0.5}Mn_{1.5}O_4$ Li-Ion Cathodes Using Water-Soluble Carrageenan as Binder.'' *J. Power Sources,* **603** 234487 (2024)
37. Burger, D. et al. ''Simultaneous Primer Coating for Fast Drying of Battery Electrodes.'' *Energy Technol.,* **13** 2401668 (2025)
38. Nikpour, M, et al. ''Li-ion Electrode Microstructure Evolution during Drying and Calendering.'' *Batteries*, **8** 107 (2022)
39. Ma, Y, Ma, J, Cui, G, ''Small Things Make Big Deal: Powerful Binders of Lithium Batteries and Post-Lithium Batteries.'' *Energy Storage Mater.*, **20** 146–175 (2019)
40. Hofmann, K, et al. ''Effect of Mechanical Properties on Processing Behavior and Electrochemical Performance of Aqueous Processed Graphite Anodes for Lithium-Ion Batteries.'' *J. Power Sources*, **593** 233996 (2024)